

OBSCURATION AND THE VARIOUS KINDS OF SEYFERT GALAXIES¹

ANDREW LAWRENCE²

Department of Physics and Center for Space Research, Massachusetts Institute of Technology

AND

MARTIN ELVIS

Harvard/Smithsonian Center for Astrophysics

Received 1981 August 13; accepted 1981 November 18

ABSTRACT

For a complete hard X-ray selected sample of active spiral galaxies we have collected luminosities of $HX = L_x$ (2–10 keV), $H\beta$ $\lambda 4861$, $[O III] \lambda 5007$, and $3.5 \mu m$ (L3.5). The effect found by Keel, that optically selected Seyfert galaxies tend to be face-on, is removed. Most of the X-ray discovered objects are “narrow emission line galaxies” (NELGs). We find that they are both selectively edge-on and lower in HX than the sample as a whole. At least some NELGs have large X-ray absorbing columns, so we believe that both the axial ratio and luminosity effects are due to obscuration. We also find that edge-on galaxies have low $H\beta/HX$; however, no effect with axial ratio is seen with $O III/HX$ or $L3.5/HX$. We thus believe that obscuration takes place in or just around the broad line region (BLR), which has a flattened configuration parallel to the disk of the parent galaxy.

We then consider a much larger sample of active galaxies of heterogeneous origin. We collect as many values as possible of HX , $SX = L_x$ (0.5–4.5 keV), $H\beta$, $O III$, luminosity at $3.5 \mu m$ (L3.5), and $10 \mu m$ (L10), and the slope of the IR continuum, α . Many values are reported here for the first time, but most are collected from the literature.

HX is the key parameter. For instance, Type 1 Seyferts, “intermediate Seyferts,” NELGs, and Type 2 Seyferts seem to form a continuous sequence of decreasing intrinsic luminosity. We find several new correlations:

1. The X-ray “hardness ratio,” HX/SX , increases smoothly for decreasing HX . We interpret this as implying that the covering factor of the BLR over the continuum source is a smooth function of HX .

2. $H\beta$ is proportional to HX , as found by other authors. On the other hand, $O III$ decreases much more slowly with decreasing HX than would be expected from a simple photoionization model. Again, we interpret this in geometrical terms: either the narrow line region also has a flattened configuration, or its filling factor of clouds is a sensitive function of either HX or the radial distance from the continuum source.

3. L3.5 is roughly proportional to HX , but L10 decreases more slowly than proportionally with decreasing HX . The power law spectral index (from Rieke) which characterizes the IR continuum from $1 \mu m$ to $10 \mu m$ is also a smooth function of HX , in that low-luminosity galaxies have steeper continua. We interpret this as meaning that the IR continuum is made up of two parts—an extension of the nonthermal continuum and thermal radiation from dust at a few hundred degrees. The slope α then characterizes the *relative* contribution of the thermal component.

4. All of these facts may be explained, at least qualitatively, if the emission line regions of Seyfert galaxies are made up of many small dense clouds, and if their filling factor (or a similar related variable) is a function of both direction and intrinsic luminosity.

Subject headings: galaxies: nuclei — galaxies: Seyfert — X-rays: sources

¹This research was sponsored in part by grants from the National Aeronautics and Space Administration under Contracts NAS8-27975 and NAS8-30751.

²Present address: Royal Greenwich Observatory, Herstmonceux, England.

I. INTRODUCTION

a) *How Many Kinds of Seyfert Galaxies Are There?*

X-ray detection of Seyfert galaxies has confused their classification. The first reports (Elvis *et al.* 1978; Tananbaum *et al.* 1978) showed that Type 1 Seyferts (i.e., those with permitted emission lines much broader than their forbidden lines) were detected at luminosities $L_x \sim 10^{42} - 10^{45}$ ergs s^{-1} (2–10 keV) whereas Type 2 Seyferts (i.e., those with permitted and forbidden lines of similar widths) were not detected, with upper limits in the range 10^{42-43} ergs s^{-1} . However, new X-ray identifications were soon made with galaxies with narrow emission lines very similar to Type 2 Seyferts and with luminosities $L_x \sim 10^{42-43}$ ergs s^{-1} (Ward *et al.* 1978; Schnopper *et al.* 1978; Bradt *et al.* 1978; Griffiths *et al.* 1979). Since five out of these seven X-ray sources were found to be variable (Ward *et al.* 1978; Marshall and Warwick 1979; Marshall, Warwick, and Pounds 1981) and since the ratio [O III] $\lambda 5007/H\beta$ was found to correlate with L_x (2–10 keV) by Griffiths *et al.* (1979), it was clear, as with Seyfert 1 galaxies, that the X-ray emission was nuclear and that photoionization was the energy input to the emission line region. This led to the suggestion (McClintock *et al.* 1979) that these NELGs (narrow emission line galaxies) were nearby Seyfert 2's and that more sensitive observations would find all Seyfert 2 galaxies to be X-ray emitters at typical luminosities an order of magnitude lower than Seyfert 1's, $\sim 10^{43}$ ergs s^{-1} . This does not seem to be the case. Recent *Einstein* observations (Kriss, Canizares, and Ricker 1980) of 14 optically selected Type 2 Seyfert galaxies detected only four and at luminosities of only $\sim 10^{41}$ ergs s^{-1} (0.5–4.5 keV). The remainder have upper limits in the range 10^{41-42} ergs s^{-1} .

What then are we to make of the NELGs? In some respects they appear to be like Seyfert 2 galaxies; in others, like Seyfert 1 galaxies. The direction of the arguments presented in this paper was influenced by several recent discoveries the importance of which will become clearer in subsequent sections.

First, Keel (1980) pointed out that known Seyfert galaxies were biased toward being face-on. We noticed, however, that several of the NELGs appear nearly edge-on (see, e.g., photographs in Wilson 1979). Second, several separate lines of evidence show that at least some of the NELGs have highly obscured nuclei (see § IIe). Third, a study by Holt *et al.* (1980) of the nearby and bright Seyfert NGC 4151 showed that, although it has a large X-ray absorbing column, the X-ray source is actually uncovered at the 10% level. They further suggested that the covering factor tended to be higher for low-luminosity Seyferts.

The above effects, and other related ones, are investigated here using two different samples. In § II we define a complete X-ray selected sample of active spirals.

This is important because of the optical selection effect noted by Keel (1980). For the 16 member galaxies, we have all of the following numbers; L_x (2–10 keV), the axial ratio of the parent galaxy, and the luminosities in [O III] $\lambda 5007$, $H\beta$, and $3.5 \mu m$ (see Table 1). The data suggest strongly that obscuration occurs in the broad emission line region, which has a flattened configuration parallel to that of the parent galaxy, and that obscuration is more likely for low luminosity objects.

In § III we consider a larger, heterogeneous sample of active galaxies. For the 69 member galaxies, we have collected as many values as possible for the following quantities; $SX = L_x$ (0.5–4.5 keV), $HX = L_x$ (2–10 keV), the luminosities [O III] $\lambda 5007$, $H\beta$, $3.5 \mu m$, and $10 \mu m$, and finally, the IR spectral index α (see Table 2). We find that the hard X-ray luminosity, HX , is the key parameter. There is direct evidence that the covering factor is a function of HX . The various “types” used previously in the literature are also a smooth function of HX . Various IR correlations further suggest that the fraction of the luminosity radiated by dust grains is a smooth function of HX . The “efficiency” with which the ionizing continuum produces O III photons is also a function of HX , suggesting that either the covering factor of the narrow emission line region is a function of HX , or possibly that the narrow line region also has a flattened configuration.

b) *Assumptions and Conventions Used throughout This Paper*

We shall assume throughout a “standard Seyfert nucleus” picture as described, for example, by Osterbrock (1978), Weedman (1977), or Davidson and Netzer (1979). This consists of a central nonthermal optical/X-ray continuum source of size less than 10^{15} cm which photoionizes the gas responsible for the strong optical emission lines. These lines come from two distinct regions: (1) the broad line region (BLR) which has density $n_e \sim 10^{9-10}$ cm^{-3} , temperature $T_e \sim 10^4$ K, and a size less than 10^{17} cm and produces the wings on the permitted lines (the breadth of these lines is assumed to be due to bulk motion of the order 10^4 km s^{-1}); (2) the narrow line region (NLR) which has $n_e \sim 10^4$ cm^{-3} , $T_e \sim 10^4$ K, and a size $\sim 10^{21}$ cm (this gas produces the forbidden lines and the narrow cores of the permitted lines, which are of width ~ 500 km s^{-1}).

It is especially important for our subsequent arguments to remember that, for both the NLR and the BLR, a comparison of the amount of matter required to explain the observed line luminosities with the densities and sizes mentioned above requires a “filling factor,” usually of $\ll 1\%$, i.e., the matter is contained in numerous small clouds or filaments. For the BLR, individual clouds may need to be extremely optically thick in order to explain the anomalous $Ly\alpha/H\alpha/H\beta$ ratios (see, e.g., Kwan and Krolik 1979).

TABLE I
COMPLETE HARD X-RAY SAMPLE OF ACTIVE SPIRALS

X-Ray Name	Type ^a	Common Name	b/a^b	Log HX	Log H β	Log O III	Log L3.5
2A0120-353	X-N	NGC 526a	0.67 ^c	43.70	40.52	41.62	30.13
2A0551+466	X-S	MCG 8-11-11	0.47	43.96	41.64	41.88	30.15
2A0710+456	O-S	MRK 376	0.68	44.60	42.65	41.87	30.84
2A0738+498	O-S	MRK 79	0.69	43.80	42.17	41.87	30.03
2A0943-140	X-N	NGC 2992	0.21 ^d	43.27	40.28	41.32	29.49
2A0946-310	X-N	MCG-5-23-16	0.63 ^c	43.21	40.04	40.95	29.52
2A1135-373	O-S	NGC 3783	0.74 ^d	43.30	41.56	41.51	29.64
2A1207+397	O-S	NGC 4151	0.74	42.88	41.38	41.74	29.23
2A1326-311	X-S	MCG-6-30-15	0.5 ^c	43.21	(40.50)	(40.34)	29.48
2A1347-300	O-S	IC 4329A	0.16	43.85	(41.76)	(41.57)	30.24
2A1348+700	O-S	MRK 279	0.68	44.27	42.15	41.68	30.11
2A1410-029	X-N	NGC 5506	0.21 ^d	43.03	40.43	41.33	29.69
2A1415+255	O-S	NGC 5548	0.83	43.68	41.97	41.88	29.95
2A2040-115	O-S	MRK 509	0.85 ^e	44.39	42.98	42.46	30.76
2A2302-088	X-S	MCG-2-58-22	0.67	44.74	43.28	42.78	30.89
2A2315-428	X-N	NGC 7582	0.33 ^d	42.57	40.30	40.83	29.30

NOTE.—Headings and units are as explained in § 1b unless otherwise noted. References may be found in Table 2. Quantities enclosed in brackets are considered uncertain (see text) and are also plotted on diagrams enclosed by brackets.

^aX = X-ray discovered; O = optically discovered; N = NELG; S = Seyfert.

^b b/a = Axial ratio. Except where noted, these values are from Keel 1980.

^cVorontsov-Velyaminov *et al.* 1962-1974.

^dDe Vaucouleurs *et al.* 1976.

^eEstimated by the authors (see text).

We shall employ the following abbreviations for quantities used frequently in graphs, tables, and text:

SX = L_x (0.5-4.5) ergs s^{-1} (soft X-ray)

HX = L_x (2-10) ergs s^{-1} (hard X-ray)

O III = luminosity in [O III] λ 5007, ergs s^{-1}

H β = luminosity in H β λ 4861, ergs s^{-1}

L3.5 = luminosity at 3.5 μ m, ergs s^{-1} Hz $^{-1}$

L10 = luminosity at 10 μ m, ergs s^{-1} Hz $^{-1}$

b/a = Holmberg estimate of axial ratio of parent galaxy

α = power law spectral index between 1 and 10 μ m after correcting for the stellar contribution (from Rieke 1978)

It is assumed throughout that HX is the least contaminated indicator of the "intrinsic" luminosity of the central ionizing source. One might then expect other properties to scale in some fashion with HX, and indeed there is much evidence that this is the case (Elvis *et al.* 1978; Kriss, Canizares, and Ricker 1980). In order to examine properties other than this simple scaling, we will normally consider correlations between values divided by HX, e.g., H β /HX versus b/a (Fig. 3). This also automatically avoids the well known problem of introducing spurious correlations with a slope of 1 between luminosities from samples with a small range of fluxes.

Throughout this work we use nonparametric statistics. Together with each graph of two quantities, we present the probability of no correlation, based on the value of the Spearman rank correlation coefficient. As we are

usually interested in the possibility of a correlation in either direction, we quote the probability based on a two-tailed test. As we present so many graphs, we expect that a reasonable acceptance level should be \sim 2% rather than the usual 5%.

II. INVESTIGATION OF A COMPLETE HARD X-RAY SAMPLE OF ACTIVE SPIRALS

a) The Axial Ratio Effect

Keel (1980) has recently demonstrated a remarkable paucity of edge-on Seyfert galaxies, i.e., those with axial ratios less than 0.5 (Fig. 1). Keel's sample of 91 Seyferts excluded elliptical galaxies as far as possible, so the effect is one of nonrecognition of edge-on spirals as Seyferts. However, Keel noted that there is no comparable effect on the nuclear visibility of normal galaxies as a function of axial ratio, so that if the effect is caused by obscuration, it is probably intrinsic to the active nucleus.

Considering the methods by which Seyfert galaxies have traditionally been discovered, nonrecognition of a weak (or weakened) Seyfert nucleus nonetheless present is essentially caused by a lack of contrast with the main galaxian body. In the X-ray waveband, however, there should be no contrast problem, so that an X-ray selected sample should have no axial ratio effect. As at least a few Seyfert galaxies are known to have large X-ray absorbing columns, we must consider a hard X-ray sample, i.e., objects selected by an experiment mostly sensitive above \sim 3 keV.

TABLE 2
EXTENDED SAMPLE

COORDINATE NAME	COMMON NAME(S)	Z	TYPE ^a	HX	SX	OIII	H β	L3.5	L10	α
0013+19	MKN 335	.025	1	43.89 (22)		41.82 (9,10,13)	42.38 (28,31)	30.52 (28,31)	30.75 (28)	0.7
0008+10	III ZW 2	.0898	1	45.08 (21)	44.88 (8)	42.75 (8,9,10, 13)	43.23 (8,9,10, 13)	31.10 (28,33)	31.18 (28)	0.4
0046+31	MKN 348	.014	2		41.62 (8)	41.50 (9,10,13)	40.39 (9,10,13)	29.51 (28,31)	30.40 (28)	2.4
0051+12	I ZW 1	.0609	1		44.26 (8)	42.46 (8,10,13)	42.80 (8,10,13)	31.25 (28)	31.70 (28)	1.2
0057+31	MKN 352	.015	1		43.49 (8)	40.62 (8,9,10, 13)	41.44 (8,9,10, 13)	29.18 (28,31)		
0113+32	MKN 1	.016	2		<41.26 (8)	41.71 (9,10,13)	40.64 (9,10,13)	29.01 (28,40)	(29.83) ^b (28)	2.3
0119-01	II ZW 1	.0541	1.5		43.32 (8)	42.53 (10)	42.44 (10)			
0120-353	NGC 526a MCG-6-4-19	.0189	N	43.7 (22)	43.0 (18)	41.62 (6)	40.52 (6)	30.13 (30)		
0120-59	F-9 ESO 113-IG-45	.0466	1	44.38 (20)		42.43 (10)	43.36 (10)	31.02 (33)		
0212-01	MKN 590	.027	1.5	43.86 (21)	43.90 (8)	41.85 (10)	41.97 (10)			
0223+31	NGC 931 MKN 1040	.0164	1	43.18 (37)		41.38 (6)	41.41 (6)			
0240-00	NGC 1068	.0036	2		41.86 (41)	42.04 (9,13,16)	40.94 (9,13,16)	30.03 (28,31)	31.01 (28)	2.2
0246+19	MKN 372 ^d	.031	1.5		42.46 (34)	42.55 (8)	41.53 (8)	29.63 (31)		
0338-01	III ZW 55	.0246	2		<41.8 (8)	41.13 (9,10,13)	40.32 (10,13)	29.33 (28)		
0430+05	3C120	.033	1	44.43 (22)	44.2 (17)	42.19 (8,9,10)	42.16 (8,9,10)	30.56 (28,29,31)	31.01 (28)	1.0
0434-10	MKN 618	.034	1		43.65 (8)	41.78 (8,10,13)	42.10 (8,10,13)			
0513-00	AKN 120	.033	1	43.96 (22)	44.15 (8)	42.20 (10)	43.04 (10)			
0517-456	Pic A	.0342	1	43.89 (21)		41.75 (38)	41.38 (38)			
0549-07	NGC 2110	.0071	N	43.05 (21.23)	41.54 (25)	41.88 (23)	41.2 (23)			
0551+46	MCG 8-11-11	.0205	1	43.96 (20)	43.41 (17)	41.88 (10,13)	41.64 (10,13)	30.15 (29)		
0710+45	MKN 376	.0553	1	44.6 (20)		41.87 (8,9,10, 13)	42.65 (8,9,10, 13)	30.84 (28,31)	31.01 (28)	0.5
0732+58	MKN 9	.0402	1		43.43 (8)	41.75 (8,9,10, 13)	42.22 (8,9,10, 13)	30.63 (28,31,40)	31.00 (28,40)	1.0
0737+65	MKN 78	.0376	2		41.88 (8)	42.48 (9,10,13)	41.38 (9,10,13)	29.84 (28)	30.89 (28)	(2.65) ^c

TABLE 2—Continued

COORDINATE NAME	COMMON NAME(S)	Z	TYPE ^a	HX	SX	OIII	H β	L3.5	L10	α
0738+49	MKN 79	.0219	1.2	43.80 (20)		41.87 (8,9,10, 13)	42.17 (8,9,10,	30.03 (28,29,31, 40)	30.53 (28,40)	1.2
0752+39	MKN 382	.034	1		43.41 (8)	41.51 (10)	41.57 (10)			
0943-14	NGC 2992	.0073	N	43.27 (20)	42.24 (18)	41.32 (2,3)	40.28 (2,3)	29.49 (33)		
0946-310	MCG-5-23-16	.0082	N	43.21 (20)	42.52 (25)	40.95 (6)	40.04 (6)	29.52 (30)		
1020+20	NGC 3227	.0033	1.2	42.23 (21)		40.51 (8,9,16)	40.18 (8,9,16, 17)	28.58 (28,29,31)	29.11 (28)	2.5
1022+51	MKN 142 ^d	.045	1		42.79 (34)	41.42 (8)	42.02 (8)			
1028+29	Ton 524a	.060	1		43.93 (8)	41.38 (10)	41.86 (10)			
1122+54	MKN 40 VV 144	.0205	1	43.78 (22)	42.86 (8)	41.09 (8,10,13)	41.31 (8,10,13)			
1129+53	MKN 176	.027	2		<41.80	41.68 (9,10,13)	40.41 (10,13)	29.92 (28,29,31)	30.39 (28)	1.3
1136-37	NGC 3783	.0091	1	43.78 (20)		41.51 (8,9,10, 11)	41.56 (8,10,11)	29.64 (28,29)	30.20 (28)	1.3
1200+44	NGC 4051	.0023	1		41.49 (25)	40.02 (13,16)	39.77 (13,16)	28.14 (28,29,31)	28.79 (28)	1.5
1206+47	MKN 198	.0241	2		<41.97 (8)	41.40 (9,10,13)	40.52 (9,10,13)	29.34 (29)	30.24 (28)	(2.15) ^c
1208+39	NGC 4151	.0033	1.5	42.88 (20)	41.52 (17)	41.74 (8,9,10, 13,16)	41.38 (13,15,16)	29.23 (28,29,31, 34)	29.82 (28)	1.45
1226+02	3C 273	.158	0	45.88 (20)	45.89 (42)	43.18 (10)	44.38 (10)	32.21 (33)		
1258+61	MKN 236	.052	1		<42.58 (8)	42.09 (10)	42.44 (10)			
1333-34	MCG-6-30-15	.0078	1	43.21 (20)		(40,34) (12)	(40,50) (12)	29.45 (12)		
1339+67	MKN 270	.009	2		<40.92 (8)	40.86 (10,13)	39.59 (10,13)	28.38 (28)		
1342+56	MKN 273	.038	2		<42.45 (8)	42.05 (13)	41.19 (13)	30.07 (28)	30.78 (28)	2.4
1346-30	IC 4329A	.0138	1	43.85 (20)		(41.57) (7)	(41.76) (7)	(30.24) (28,29,33)	30.8 (28)	
1351+69	MKN 279 ^e	.0307	1	(44.27) ^e (20)		41.68 (9,10,13)	42.15 (9,10,11 13)	30.11 (28)	30.49 (28)	1.4
1353+38	MKN 464	.0512	1	44.47 (21)		42.17 (10,13)	42.08 (10,13)			
1354+19	MKN 463	.0505	2		<42.41 (8)	42.88 (13)	42.08 (13)			

TABLE 2—Continued

COORDINATE NAME	COMMON NAME(S)	Z	TYPE ^a	HX	SX	OIII	H β	L3.5	L10	α
1410-02	NGC 5506	.0061	N	43.03 (20)	42.13 (18)	41.33 (5)	40.43 (5)	29.69 (32)		
1415+25	NGC 5548	.0166	1.5	43.68 (20)	43.40 (17)	41.88 (8,9,10, 13,16)	41.97 (8,9,10, 11,13,16)	29.95 (28,29,31)	30.40 (28)	1.0
1433+40	MKN 474	.044	1		43.41 (8)	41.66 (10,13)	41.81 (10,13)			
1439+53	I ZW 92	.0374	2		<42.11 (8)	42.8 (10,13)	41.88 (10,13)			
1534+58	MKN 290	.0308	1		43.80 (8)	42.03 (8,10,13)	42.22 (8,10,13)	29.94 (31)		
1535+54	MKN 486	.039	1		<42.30 (8)	41.64 (8,10,13)	42.30 (8,9,10, 13)	30.30 (28,31)	30.61 (28)	0.8
1552+19	MKN 291	.035	1		43.32 (8)	41.86 (8,10,13)	41.18 (8,10,13)			
1659+29	MKN 504	.036	1		43.28 (8)	41.48 (10)	42.06 (10)	29.72 (31)		
1720+30	MKN 506	.0433	1.5		43.79 (8)	41.87 (8,10,13)	41.86 (8,10,13)	30.10 (28,31)		
1748+68	MKN 507	.053	2		42.91 (8)	(40.86) (26)	(40.95) (26)			
1833+32	3C 382	.0586	1	44.78 (21)	44.40 (8)	42.12 (8,10,13)	42.84 (8,10,13)	30.73 (39)	30.78 (39)	
1845+79	3C390.3	.057	1	44.69 (22)		42.51 (8,10,13)	42.59 (8,10,13)			
1906+50	NGC 6764	.0082	2		<40.93 (8)	39.87 (10)	40.17 (10)	28.50 (28)	29.64 (28)	3.5
1914-58	ESO 141-G55	.0369	1	44.08 (20)	44.15 ^f (17)	41.80 (10)	42.50 (10)	30.67 (33)		
193P-10	NGC 6814	.0053	1	42.6 (20)	41.34 (17)	40.22 (13)	39.73 (13)	28.54 (28,33)	28.83 (28)	2.2
2041-10	MKN 509	.0352	1	44.39 (20)		42.46 (8,10,13)	42.98 (8,10,13)	30.76 (28,31,33)	30.87 (28)	0.6
2214+13	MKN 304	.0665	1		43.34 (8)	42.02 (8,10,13)	42.95 (8,10,13)	30.77 (28,31)	31.14 (28)	1.1
2251-17 ^g	MR 2251-17 ^g	.068	0	44.91 (20)	44.49 (42)	43.08 (43)	43.27 (43)	30.77 (33)		
2300+08	NGC 746 ^g	.0167	1	43.83 (20)		41.92 (8,9,10, 13,16)	42.10 (8,9,10, 13,16)	30.34 (28,31,33)	30.86 (28)	1.4
2301+22	MKN 315	.0395	1.5		42.96 (8)	41.97 (8,10)	41.69 (8,10)	30.06 (28)	30.66 (28)	1.8
2302-088	MKN 926 MCG-2-58-22	.0475	1	44.74 (20)		42.78 (36)	43.28 (1)	30.89 (33)		
2315-42	NGC 7582	.0049	N	42.57 (20)	41.23 (18)	40.83 (3)	40.30 (1,3)	29.30 (33)		
2353+07	MKN 541	.0419	1	43.92 (22)		41.44 (10)	42.09 (10)			

(Notes) on following page

NOTES TO TABLE 2

Headings and units as defined in § 1b.

Numbered references to each value are enclosed in brackets beneath the value and refer to the list following these notes.

Quantities enclosed by brackets are considered uncertain (see text), and are also plotted on diagrams enclosed by brackets.

^aIntermediate types from Osterbrock 1977.

^bNeugebauer *et al.* 1976 give L10 = 30.47.

^cCalculated by the authors using L10 and L3.5 corrected for galaxy contamination by Kriss, Canizares, and Ricker 1980.

^dThese two *HEAO A-2* candidates were almost certainly mis-identifications. This information, and the correct values of SX, privately communicated by Kriss.

^eThe identification of MRK 279 with 2A 1348+700 has been disputed by Dower *et al.* 1980. The value of HX used here seems consistent on all of our diagrams, however.

^fIn this observation we did not detect the very large soft X-ray excess observed by Mushotzky *et al.* 1980.

REFERENCES TO TABLE 2

- 1) Ward *et al.* 1978.
- 2) Osmer, Smith, and Weedman 1974.
- 3) Ward *et al.* 1980.
- 4) Shuder 1980.
- 5) Wilson *et al.* 1976.
- 6) M. Ward, private communication.
- 7) Wilson and Penston 1979.
- 8) Kriss, Canizares, and Ricker 1980.
- 9) Adams and Weedman 1975.
- 10) Steiner 1981.
- 11) Elvis *et al.* 1978.
- 12) Pineda *et al.* 1980.
- 13) Yee 1980.
- 14) Osterbrock 1977.
- 15) Boksenberg *et al.* 1975.
- 16) Anderson 1970.
- 17) This paper.
- 18) Maccacaro *et al.* 1982.
- 19) Stark *et al.* 1978.
- 20) Cooke *et al.* 1978.
- 21) Marshall *et al.* 1979.
- 22) Tananbaum *et al.* 1978.
- 23) McClintock *et al.* 1979.
- 24) Elvis 1978.
- 25) F. E. Marshall, private communication.
- 26) Koski 1978.
- 27) Stocke *et al.* 1982.
- 28) Rieke 1978.
- 29) McAlary *et al.* 1979.
- 30) I. Cruz-González, private communication.
- 31) Stein and Weedman 1976.
- 32) Glass 1978.
- 33) Glass 1979.
- 34) G. Kriss, private communication.
- 35) Penston *et al.* 1974.
- 36) Ward 1979.
- 37) Ward and Wilson 1978.
- 38) Danziger *et al.* 1977.
- 39) Puschell 1981.
- 40) Neugebauer *et al.* 1976.
- 41) W. Ku, private communication.
- 42) Ku *et al.* 1980.
- 43) Canizares *et al.* 1978.

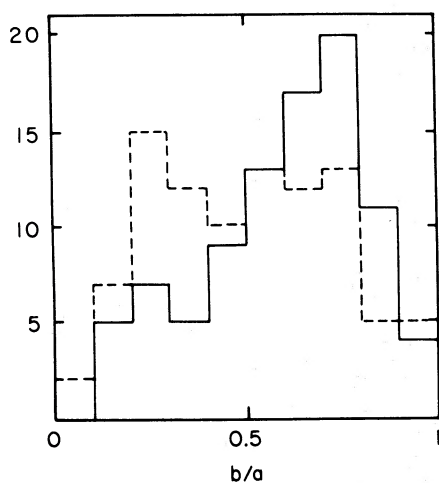


FIG. 1.—Distribution of axial ratios for 91 Seyfert (solid line) and comparison (dashed line) galaxies. From Keel (1980).

b) Definition of the X-Ray Sample

Warwick and Pye (1979) have defined a subset of the 2A catalog (Cooke *et al.* 1978) to be a complete sample of extragalactic X-ray sources brighter than 0.6 SSI counts s^{-1} (3×10^{-11} ergs $cm^{-2} s^{-1}$, 2–10 keV) at $b^{II} > 10^\circ$. The sample contains 23 “active galaxies”—11

Seyfert galaxies, 2 QSOs, 3 BL Lacertae objects, 1 radio galaxy, and 6 NELGs. Ward *et al.* 1978) suggest that identifications of this sample are complete for galaxies down to ~ 16 th magnitude. The 10 unidentified sources remaining in the 2A sample are likely to be cataclysmic variable stars (McHardy *et al.* (1981). The optically active nature of 10 of the 23 objects was first discovered by examining candidate optical objects inside the X-ray error box.

From the 23 objects we selected those satisfying the following criteria: (1) The object is accepted to be a galaxy. This conservatively excludes the QSOs and 2 of the 3 BL Lac objects. (2) The object is not an elliptical galaxy. This excludes NGC 5128 and Mrk 421. (3) The X-ray emission comes from an active nucleus in the galaxy. This excludes M82, for which there is recent evidence (Watson and Griffiths 1980) that the X-ray source is extended. M82 is also considerably less luminous than all other objects in the potential list.

The resulting sample of 16 active spirals is listed in Table 1, together with HX, b/a , O III, $H\beta$, L3.5, and a “type.” The luminosities are derived as explained in § III for Table 2.

The axial ratios are all estimates in the sense of Holmberg (1975). Where possible they are from Keel (1980); otherwise they are from the *Reference Catalogue*

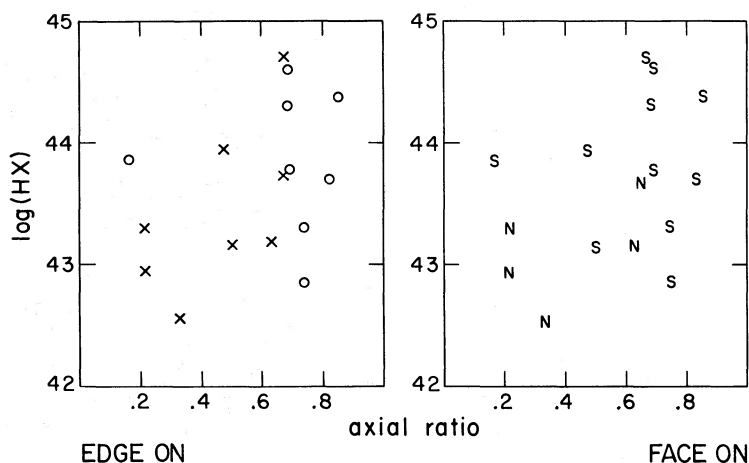


FIG. 2.—Complete sample. Distribution in HX and b/a . The data are plotted twice, to show two different divisions into two groups. On the left, O = optically discovered, X = X-ray discovered. On the right, S = Seyfert galaxy, N = NELG.

of *Bright Galaxies* (de Vaucouleurs, de Vaucouleurs, and Corwin 1976) or the *Morphological Catalogue of Galaxies* (Vorontsov-Velyaminov *et al.* 1962–1974), except for Mrk 509, whose axial ratio has been estimated by the authors from the plate in Adams (1977). Photometric diameters are provided in de Vaucouleurs, de Vaucouleurs, and Corwin (1976); these have been “uncorrected” using the table in Holmberg (1975), so that they are compatible with the other values, which are all Holmberg estimates.

c) Distribution of the Sample in HX and b/a

Figure 2 shows the X-ray luminosity and the axial ratio for each of the galaxies. They are plotted twice, first divided into those that were discovered by optical methods and those discovered by the X-ray survey, and second divided into those that have been called Seyfert galaxies and those that have been called narrow emission line galaxies. We have tested the proposition that these various groups were drawn at random from the same parent population, for the distributions of both HX and b/a . We used the nonparametric Mann-Whitney U -test. This is a one-tailed test, so we can verify the direction of any difference between populations (see, e.g., Siegel 1956).

The results can be summarized as follows. At the 0.5% level, X-ray discovered objects have smaller b/a than optically discovered objects. However, there is no difference in the HX distribution for these two populations. Next, considering NELGs versus Seyferts, we can state at the 2.5% level that NELGs have both lower b/a and lower HX. We emphasize that we can study the separate dependencies on HX and b/a , as, for the complete sample, we find that there is no correlation between these two quantities.

Unfortunately, we have no comparison sample, so we cannot strictly state that the X-ray selected sample completely removes the optical selection effect noted by Keel (1980). Nonetheless it seems most likely that it is optical obscuration that produces Keel’s result. Half the Seyfert galaxies have been hiding, and now X-ray detectors are finding them.

d) Clues to the Location of the Obscuring Region

Figure 3 presents $H\beta/HX$, $O\text{ III}/HX$, and $L3.5/HX$ against b/a for the complete sample. The probability of there being no correlation is shown in the corner of each graph. It appears that edge-on galaxies have relatively little $H\beta$ for their X-ray luminosity. There is no correlation against axial ratio for either $O\text{ III}/HX$ or $L3.5/HX$.

This has immediate consequences for the nature and geometry of the obscurer. The lack of correlation with $L3.5/HX$ suggests that obscuration is caused by reddening if we assume that $L3.5$ represents the nonthermal continuum (see § III d). The lack of correlation with $O\text{ III}/HX$ suggests that the reddening occurs in or just outside the BLR; and consequently that the BLR or the immediately surrounding region has a flattened configuration, parallel to the disk of the parent galaxy. Alternatively, the reddening may occur in the body of the parent galaxy, if the NLR has a much larger scale height than the obscuring material in the parent galaxy. However, Keel (1980) has pointed out that there is no axial ratio effect on the visibility of the nuclei of normal galaxies, whose nuclear scale heights are comparable with their parent disks.

Here we are only able to consider the total luminosity in $H\beta$; ideally we should consider broad and narrow components separately.

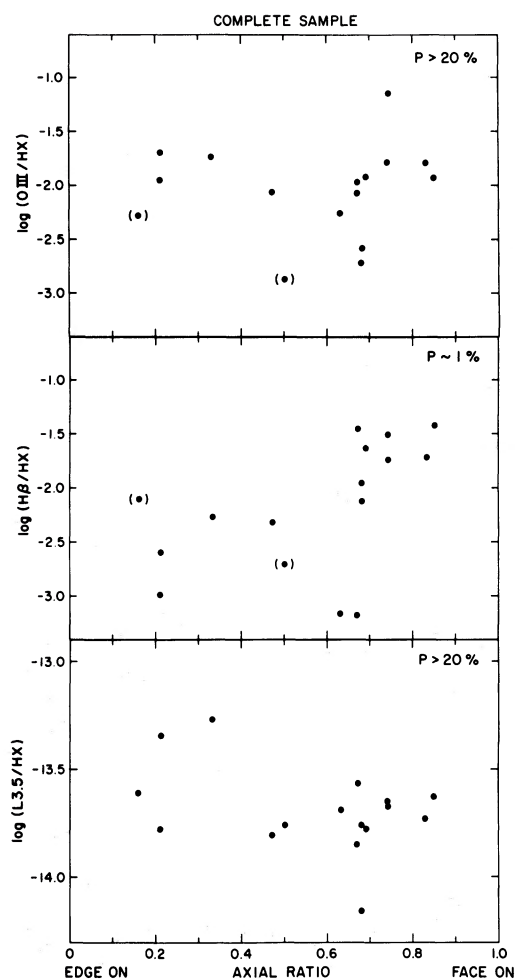


FIG. 3.—Complete sample: Behavior of the sample as a function of axial ratio, b/a .

e) Narrow Emission Line Galaxies as Obscured Type 1 Seyferts

Evidence is accumulating of obscuration in NELGs.

1. NGC 5506, NGC 7582, NGC 2992, NGC 2110, and MCG-5-23-16 all have large X-ray absorbing columns, of the order $N_{\text{H}} \sim$ several times 10^{22} cm^{-2} (Stark, Bell Burnell, and Culhane 1978; Maccacaro, Perola, and Elvis 1982; Mushotzky 1982), unlike most classical Seyferts (Mushotzky *et al.* 1980).

2. The first three of these galaxies also have a very large IR luminosity ($\sim 10^{44} \text{ ergs s}^{-1}$, Glass 1978, 1979).

3. Observations by Ward of NGC 526a (unpublished, but quoted in Griffiths *et al.* 1979) show the $\text{H}\alpha$ emission line to have faint but very wide wings, whereas $\text{H}\beta$ has no wide wings, indicating that a broad line region exists in this galaxy but is heavily obscured and reddened. Shuder (1980) and Véron *et al.* (1980) also find that NGC 2110, NGC 2992,

NGC 5506, and MCG-5-23-16 have faint very wide wings on $\text{H}\alpha$, but not on $\text{H}\beta$. Phillips *et al.* (1979) found the HEAO A-2 X-ray source ESO 103-G35 to have a very similar optical spectrum.

If the absorbing gas in NELGs has a dust-to-gas ratio like that found in our Galaxy, an X-ray column density of $5 \times 10^{22} \text{ cm}^{-2}$ predicts $A_v = 20 \text{ mag}$ (Jenkins and Savage 1974). This is sufficient to remove even a fairly luminous broad $\text{H}\beta$ line. Calculations which attribute the discrepancy between the ratio of observed $\text{H}\alpha/\text{H}\beta$ and the expected recombination value, to reddening, yield much smaller values of A_v when only the narrow components are considered (Maccacaro, Perola, and Elvis 1982). A likely explanation is that the NLR is external to the obscuring region. The lack of detection of broad $\text{H}\beta$ means that only a lower limit may be placed on the value of A_v appropriate to the BLR. However, Maccacaro, Perola, and Elvis (1982) find that at least in two cases (NGC 2992 and NGC 5506) A_v for the BLR is significantly larger than A_v for the NLR. There is a problem with this picture in that, in the case of NGC 7582, the 2200 \AA absorption feature implies a much smaller effective A_v for the UV continuum. As suggested by Maccacaro, Perola, and Elvis (1982), this may require that a large part of the UV continuum originate outside the obscuring region (e.g., in hot stars) or, quite feasibly, that the size distribution and composition of the dust, or the gas to dust ratio, be different from that found in our local interstellar medium.

These considerations lead naturally to the suggestion (e.g., Véron *et al.* 1980) that all so-called narrow emission line galaxies may be obscured Type 1 Seyferts. The possibility also suggests itself that Type 2 Seyferts are extreme examples of this phenomenon. This question is explored in the next section.

We have ascertained that there may be two reasons for obscuration—an axial ratio effect and a luminosity effect. For the examination of effects with b/a , the complete sample is essential. However, in further investigation of luminosity effects, we may benefit by having a much larger sample, even if the members have been chosen in an ill-defined manner.

III. INVESTIGATION OF A LARGE HETEROGENEOUS SAMPLE OF SEYFERT AND RELATED GALAXIES

a) The Sample

We have collected a large number of X-ray, optical, and IR luminosities for galaxies observed either by various hard X-ray experiments (*Uhuru*, *Ariel 5*, *HEAO 1*), or the IPC on the *Einstein* satellite (Table 2). Some of these measurements are new, and were made by the authors; some are new, and are private communications from various colleagues; but most have been collected from the literature. Where several values are available, we have taken an average, except in the case of large

discrepancies, which have been noted. We do not expect that the list is comprehensive, but it is close to being so. Two specific points are necessary.

All values of SX have assumed a power law of spectral index -0.5 , and a column density as expected from our own Galaxy. Very few of the detections have enough photons to make any comment about the presence of low-energy cutoffs, or substantially different slopes.

For emission line measurements, we had the following order of preference. (1) Absolute spectrophotometry using a slit of width greater than $5''$. (2) Line ratios and equivalent widths from narrow-slit spectra (e.g., Osterbrock 1977) used together with wide-slit, low-resolution absolute spectrophotometry (e.g., de Bruyn and Sargent 1978). (3) Direct measurement of a line from published wide-slit, low-resolution spectrophotometry. These last two methods have been used extensively by Kriss, Canizares, and Ricker (1980), Yee (1980), Steiner (1981), and occasionally by the authors. (4) If no other measurement was available, we accepted a narrow-slit measurement, but bracketed both the tabulated values and the plotted points.

We have also listed α , the IR spectral index, taken from Rieke (1978). Rieke obtained this number by fitting a combination of a power law of index α , and a 3500 K blackbody, to the IR spectrum between 1 and 10 μm . The index α is thus a characterization of the steepness of the IR continuum after correction for galaxian contamination.

In the next few sections, we discuss various results from this sample. In § IV we attempt to draw the separate strands together a little.

b) X-Ray Hardness Ratio and the Covering Factor of the BLR

Only a handful of galaxies have been measured both by hard and soft X-ray experiments, but already an important fact is apparent. Figure 4 shows HX/SX against HX for our sample. Low-luminosity galaxies have relatively large hardness ratios. As several of these are known to have large X-ray absorbing columns (e.g., Maccacaro, Perola, and Elvis 1982; Mushotzky 1982) whereas many of the high-luminosity galaxies are known not to have large columns (Mushotzky *et al.* 1980), it would seem likely that the effect is always one of an increasing deficit of soft X-rays in lower luminosity galaxies.

A similar effect has been pointed out by Mushotzky (1982), who finds a correlation between HX and the measured column density N_{H} for a mixed sample of Seyferts and NELGs. Note that above $\text{HX} = 10^{44}$ ergs s^{-1} the curve seems to flatten out near the value expected for a pure power law of energy index 0.5, and that below this the curve is smooth—it is not a change of state at some critical luminosity. In the context of the discovery by Holt *et al.* (1980) that the X-ray source in

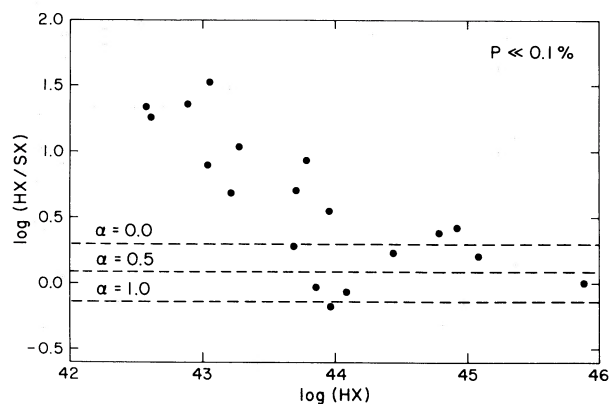


FIG. 4.—Extended sample: X-ray “hardness ratio” HX/SX plotted against HX. The dotted lines represent the values expected for energy power laws of slope $\alpha = 1, 0.5$, and 0.0 .

NGC 4151 is unobscured at the 10% level, and the evidence discussed in § IIe that obscuration occurs in the BLR, the best explanation for Figure 4 must be that the covering factor of the BLR over the X-ray source is a smooth function of HX. If we make the simplifying assumption that some regions of the X-ray source are completely obscured in the SX band, but completely unobscured in the HX band, then $\log(\text{HX}/\text{SX}) = 1.5$ corresponds to an uncovered fraction of $\sim 4\%$ for an underlying power law spectrum of energy index 0.5. This is necessarily a crude approximation as, for instance, the two X-ray bands overlap, but it is a useful first estimate.

Two further points should be made. First, note that in the following graphs of other properties of the sample, the consistently different slopes of the SX and HX versions of the same graph act as independent confirmation of the hardness ratio effect for a much larger sample of galaxies than is directly available for Figure 4. Second, there probably are some anomalies. If marginal (4σ) HX detections of NGC 1068 and Mrk 486 reported by Elvis (1978) are real, then neither of these galaxies will fit the relation. Mrk 486 has SX a factor 50 lower than would be expected either from our HX/SX relation or from its large $\text{H}\beta$ luminosity. NGC 1068 has HX a factor 10 smaller than would be expected from the HX/SX relation, although we also note that it is below the range so far covered by the relation.

We have also examined (but have not plotted) all those objects that have available measured SX, and an upper limit to HX from Elvis *et al.* (1978). None of these limits are useful, except, seemingly, for Mrk 618, which appears to strongly violate the relation. However, we have ascertained that the limit to HX is in error. The flux limit quoted by Elvis *et al.* (1978) is correct; conversion to luminosity using the known redshift of Mrk 618 yields a limit to HX three orders of magnitude larger than that quoted in Elvis *et al.* (1978).

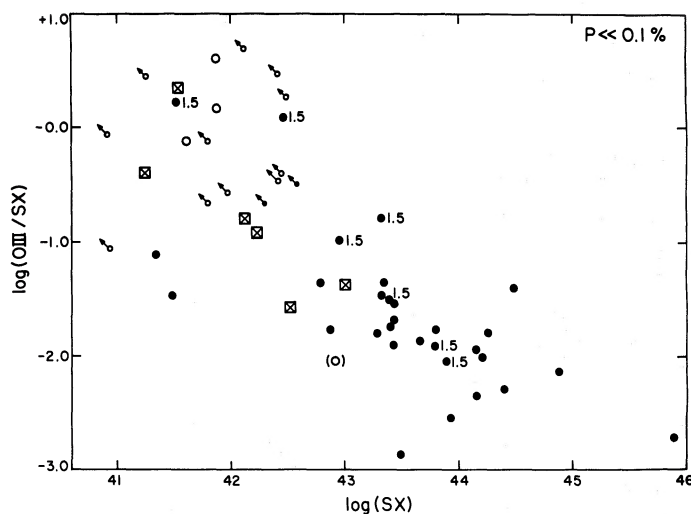


FIG. 5.—Extended sample: O III/SX against SX. Symbols: ●, Type 1 Seyfert. ○, Type 2 Seyfert. ⊠, NELG. ●1.5, Intermediate Seyfert. In this graph and others, galaxies detected in X-rays have deliberately been drawn as slightly larger symbols than those that have only upper limits.

c) *The Continuity of Types and the “Efficiency” of NLR and BLR*

Measurements of Seyfert galaxies by the *Einstein Observatory* have now covered a very large range in luminosity. This makes the relationship between various types somewhat clearer. Figure 5 shows O III/SX against SX, with various “types” indicated by different symbols. The four groups—Type 1, intermediate, NELG, and Type 2—are each seen to occupy about 2–3 decades of luminosity in successively lower ranges. Although there is a very large overlap, it is clear that the dominant factor in deciding the “type” of a Seyfert galaxy has been the (usually unknown) X-ray luminosity. Most of the upper limits on Type 2’s (from Kriss, Canizares, and Ricker 1980) are also consistent with their being low-luminosity Type 1 Seyfert galaxies. The low value of O III/HX in NGC 3227 and NGC 6814 is the reason why these low-luminosity galaxies have been classified as Type 1 rather than Type 1.5—broad H β is very weak, but so is narrow H β , so that there is not a distinct “core plus wing” structure. In all the rest of our plots we make no distinction between the various kinds.

Figure 5 also shows that low-luminosity types have relatively large O III for their X-ray luminosity. Figure 6*b* demonstrates this for O III/HX against HX. Note that the slopes of the hard and soft X-ray versions are not the same. This is because of the hardness ratio effect (Fig. 4), that HX and SX do not simply scale. As noted before, HX must be seen as the truest indicator of “intrinsic” luminosity, but in this case the correlation of O III/SX with SX is physically more enlightening. SX represents that part of the soft X-ray luminosity which escapes the BLR to the viewer; likewise it represents that part of the ionizing continuum which is capable of

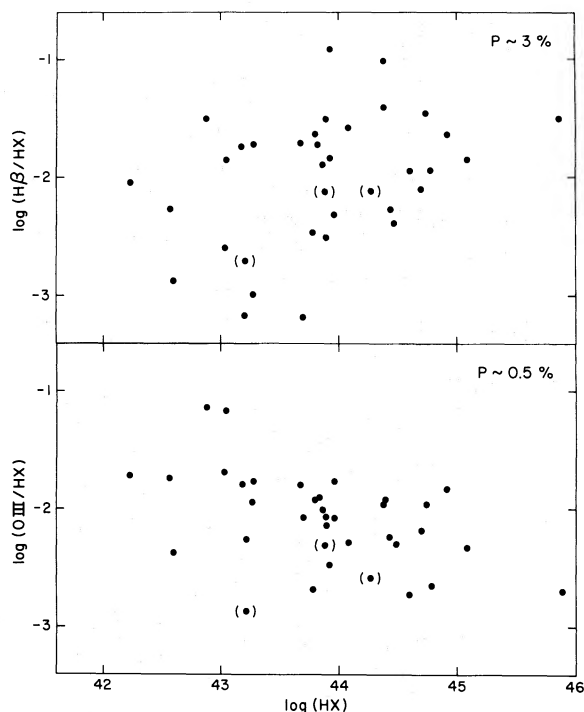


FIG. 6.—Extended sample: (a) H β /HX against HX. (b) O III/HX against HX.

ionizing the NLR. Then, assuming there is no slope change from SX to the UV as a function of luminosity, O III/SX represents the number of O III photons created per ionizing photon, i.e., the “efficiency” of the NLR.

It might be objected that the observed slope of about -1 suggests that O III is merely independent of SX; mathematically this is correct, but physically it is mis-

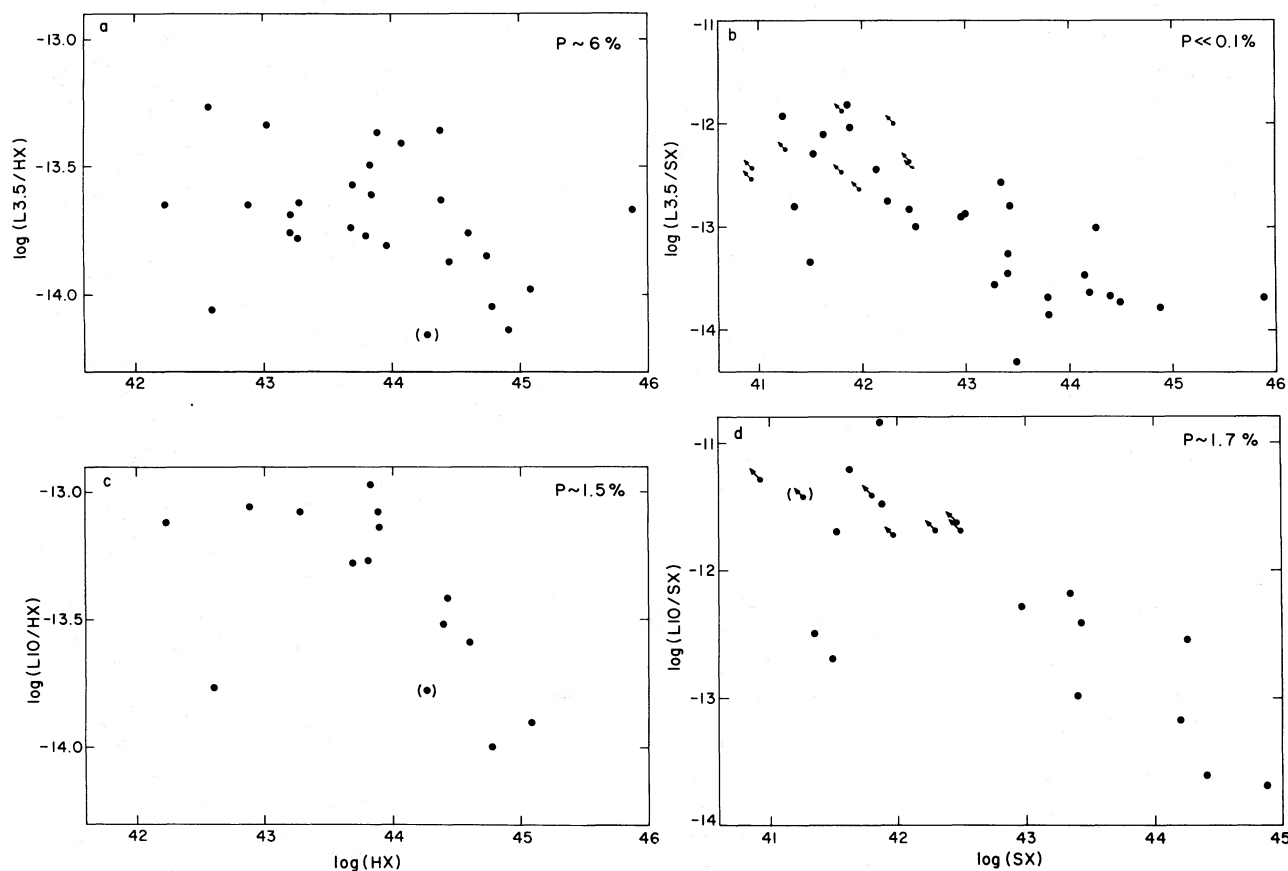


FIG. 7.—Extended sample: L10 and L3.5 scaled and plotted against HX and SX in turn

leading. O III is not independent of HX, and thus is related to the intrinsic overall luminosity. We have also verified that O III correlates directly with SX.

Figure 6a shows $H\beta/HX$ against HX. There is a marginal but slow correlation in the sense that low-luminosity galaxies have a relatively small $H\beta$ efficiency. However, the scatter is large, and any correlation present does not deviate strongly from proportionality of $H\beta$ to HX.

d) IR "Efficiency" and the Relative Amount of Dust

Discussing an IR "efficiency" is not so simple, as it is not clear whether the IR continuum should be considered as originating from the central source, or as reprocessed radiation of some sort, e.g., heated dust. We shall argue that it is both. This has been suggested previously by several authors (e.g., Rieke 1978). We also, however, present evidence that the relative contribution of dust is a smooth function of HX.

Figure 7 shows L3.5 and L10 scaled to both SX and HX. As noted before, HX should be considered fundamental, and the difference in slope between HX and SX

versions is purely a consequence of the hardness ratio effect (Fig. 4). However, it is worth examining both, as there are few galaxies that have both HX and SX measurements available. In particular, Type 2 Seyferts have so far been measured only with the IPC on *Einstein* (Kriss, Canizares, and Ricker 1980). SX versions should then be seen as confirmation and extension of correlations seen in HX graphs.

L10 efficiency correlates quite steeply with both HX and SX. There is no strong evidence for a correlation of L3.5 efficiency with HX; L3.5 efficiency correlates with SX, but this may be purely a result of the hardness ratio effect (Fig. 4). Whether or not this is the case, it is clear that L10 efficiency is a steeper function of HX than L3.5 efficiency, which must mean that the shape of the IR continuum is a function of HX.

This may easily be the result of mixed dust and nonthermal contributions. Dust cannot survive at temperatures above ~ 1000 K, and thus will radiate almost entirely longward of $1 \mu\text{m}$. A thermal spectrum will peak near $10 \mu\text{m}$ for a temperature of a few hundred kelvins. Thus it is likely that L3.5 measures a nonthermal component which simply scales to HX whereas L10

measures mainly a thermal component at a few hundred kelvins which scales more slowly. Note that L10 is not independent of HX; this is not simply a thermal source present in the nuclear region but unconnected with the active nucleus.

Another complication, serious at $3.5 \mu\text{m}$ but not at $10 \mu\text{m}$, is that the relative contribution of the parent galaxy will be larger for low-luminosity nuclei. For a large number of Seyfert galaxies, Rieke (1978) has fitted the IR continuum between 1 and $10 \mu\text{m}$ with two contributions; a 3500 K blackbody, representing the stellar contribution, and a power law of index α representing the contribution of the active nucleus. Rieke (1978) noted that Type 2's as a class have a larger mean α , and he suggested that this is because they contain substantial amounts of dust. It also seemed that some Type 1's have a lot of dust, whereas others seem purely nonthermal.

In Figure 8 (α versus HX and SX) we see that in fact α is a smooth function of HX. As L3.5 is close to being proportional to HX, we interpret this as meaning that while there is a nonthermal IR continuum in all Seyferts that simply scales to HX, there is also a thermal component that scales less steeply with HX and that is increasingly important at longer wavelengths. We may identify this thermal IR component with the gas and accompanying dust required to produce the X-ray column and remove the broad emission lines. We note that if this thermal component has a mass larger than that expected for the BLR ($\sim 10^{1-2} M_{\odot}$) but smaller than that expected for the NLR ($\sim 10^{4-6} M_{\odot}$) and if it has a size larger than that of the BLR ($\sim 1 \text{ pc}$), then its blackbody cooling time at a temperature of several hundred kelvins cannot be greater than a few months. It is then required that the thermal IR component be also continuously energized in some fashion.

IV. DISCUSSION

a) Immediate Conclusions

We have arrived at several observationally compelling conclusions: (1) Various classes of active galaxies form a smooth sequence of properties with X-ray luminosity (HX) as the fundamental parameter. (2) The BLR, or a region just outside it, is the source of obscuration in Seyfert galaxies. (3) The BLR or surrounding region has an oblate distribution, which is flattened in the same sense as the parent galaxy. (4) The covering factor of the continuum source by the BLR is a smoothly decreasing function of HX. (5) The efficiency with which the NLR intercepts ionizing photons and converts them into O III emission line photons decreases with HX. (6) The fraction of the total luminosity contributed by thermal radiation from dust grains is a smoothly decreasing function of HX. (7) HX is clearly the dominant variable. However, the large scatter on most correlations tells us that at least one other independent parameter must be involved.

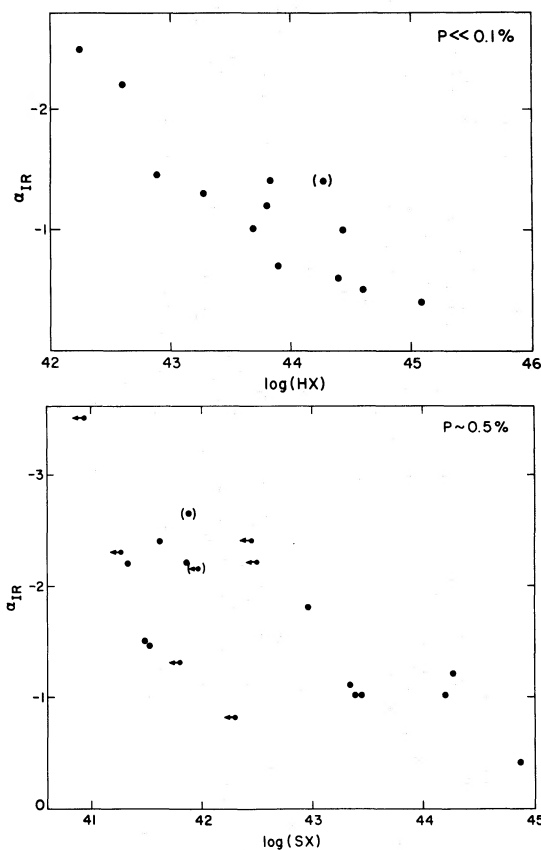


FIG. 8.—Infrared spectral index α , as a function of HX and SX.

Several questions come to mind. Why should the covering factor be a function of HX? Why is HX the prime variable? Are *all* Type 2 Seyferts really obscured Type 1 Seyferts? These questions and others are explored in § IVc. First, however, we shall go beyond our initial conclusions and make some less certain but very plausible deductions concerning the physical conditions and geometry of the emission line regions.

b) Plausible Deductions

i) The Geometry of Obscuration by the BLR

Previous work has established some reasonably firm conclusions concerning the BLR clouds. BLR filling factors are usually less than 1%. The clouds are mostly composed of gas at a density of $n_e \sim 10^{9-10} \text{ cm}^{-3}$, as shown by the absence of broad forbidden lines but the presence of broad semiforbidden C III] $\lambda 1909$. There are probably many small clouds rather than a few big ones (Carswell and Ferland 1980; Davidson and Netzer 1979), so that covering factor is a well defined quantity. However, they are large enough to be optically thick to $\text{H}\beta$ (Kwan and Krolik 1979), requiring a column of $\gtrsim 10^{22} \text{ cm}^{-2}$. We may then reasonably expect them to be of

thickness $R = 10^{12-13}$ cm. Each cloud is optically thick to X-rays through most of the *Einstein* IPC band.

The above estimates suggest the following simplified picture, which may clarify further discussion. The broad line region may be crudely imagined as a swarm of glowing marbles. Possibly the structure may be more filamentary or sheetlike. However, unless cloud motions are highly ordered, the large velocities of individual clouds probably means that they are topologically disconnected regions.

We assume that the central X-ray source is much smaller than the BLR, but much larger than an individual marble. Each marble exposed to the central source is heated by it and glows uniformly in $H\beta$ photons. Some marbles are in the shadow of others and can cool. Viewed from a distance, imagine the X-ray source to be divided into many elements of size smaller than the marbles. The column density of marbles through the BLR is such that, on average, each element is covered by N marbles. The X-ray absorbing column density is proportional to N ; the effective X-ray cutoff energy $E_a \propto N^{3/8}$. The exact effect on the HX and SX bands is then quite complicated, but a first order comprehension may be gained if we assume that HX is unaffected by the marbles, whereas one or more marbles covering an element reduces the contribution to SX from that element to zero. We expect this to be a reasonable assumption for columns up to $\sim N_H = 10^{24}$ cm $^{-2}$ at which point HX begins to be substantially affected by absorption. The probability of no marbles covering an element is e^{-N} , assuming Poisson statistics. A fraction e^{-N} of the elements will be uncovered so that $SX(\text{observed}) = SX(\text{intrinsic}) \times e^{-N}$. A prediction of this simple picture is that on average the mean X-ray absorbing column density N_H should be inversely proportional to the logarithm of the uncovered fraction.

All marbles are optically thick to SX. Only hot marbles are sources of $H\beta$. Only cool marbles, which contain dust, are optically thick to the wings of $H\beta$, and radiate thermally at a few hundred kelvins. As the marbles are moving, cool marbles will occasionally glimpse the X-ray source which thus energizes the $10 \mu\text{m}$ continuum. As N is a function of radial distance from the X-ray source, so also will be the relative amounts of time a marble will spend as an $H\beta$ emitter or as a thermal IR emitter.

The relations between HX, SX, $H\beta$, and L10 which we have described in this paper may then be explained, at least qualitatively, if N is a function of both direction and intrinsic luminosity, $N = N(\theta, \phi, HX)$. For a uniform distribution of clouds of one size, r , and number density, n , seen through thickness H , we find $N = nr^2H$. Alternatively, in terms of the filling factor f , $N = fH/r$. As the uncovered fraction = e^{-N} , it is very sensitive to variations in N if N varies in the range 0.1–5 and very insensitive outside this range. This corresponds to HX ranging from $\sim 3 \times 10^{44}$ ergs s $^{-1}$ to $\sim 3 \times 10^{42}$ ergs s $^{-1}$.

Above this range the BLR is essentially totally uncovered, whereas below it the BLR is completely covered, probably in all directions. We might then expect no axial ratio effect for Type 2 Seyferts alone—as has been suggested to be the case by Keel (1980). In the intermediate range observed properties are a sensitive function of both luminosity and inclination. $H\beta$ will remain approximately proportional to HX. As the covering factor increases, a larger fraction of the ionizing continuum will be intercepted; but to first order the covering factor of the BLR over itself is the same as the covering factor of the BLR over the continuum, so that a similarly larger fraction of $H\beta$ photons will not escape the BLR. Meanwhile a larger fraction of the BLR marbles will radiate as cool, dust bearing, marbles rather than as hot, emission line, marbles.

ii) *Geometry of the NLR*

Regardless of the value of SX(intrinsic) and its reduction by BLR clouds, the fact that O III/SX(observed) is large for small SX(observed) implies that the NLR is more “efficient” for low luminosity galaxies. We can present several plausible geometrical reasons for this:

1. The covering factor ($= fH/r$) of the NLR over the central ionizing source is also a function of HX.

2. The overall structure of the NLR is not a function of HX but the factor f/r (filling factor over cloud size) is a decreasing function of R , the radial distance from the X-ray source. This relies on the fact that both the inner and outer radius of the zone of O $^{++}$ (the “Strömrgren shell”) depend on the luminosity of the ionizing source. The luminosity in [O III] $\lambda 5007$ depends on the rate of collisional excitation of the necessary excited state (which depends on T_e and n_e) and the number of O III atoms. The temperature is fixed near $T_e = 10^4$ K by the balance between photoionization and cooling. In a simple model where all clouds are the same size and density, the recombination time and collisional excitation time are constant, whereas the ionization time varies as SX/R^2 . The volume of the O III shell then varies as $SX^{3/2}$. To achieve the O III efficiency effect (Fig. 5) then requires that the local filling factor f varies as something like R^{-3} . In general fn_e/r may be a steeply decreasing function of R .

3. The NLR may also have a flattened configuration. In this case, for sufficiently luminous galaxies, the Strömrgren radius for O $^{++}$ will exceed the scale height of the NLR. The NLR gas then subtends only a small solid angle from the ionizing source. For low-luminosity galaxies, the potential O III shell may be entirely contained within the actual NLR. A similar point has been made by Steiner (1981) with respect to a correlation found between O III/ $H\beta$ and $H\beta$ for a sample of low-redshift quasars and Seyfert galaxies. It may also be that the axial ratio of an oblate configuration of both the NLR and the BLR is a function of HX in that high-luminosity objects are more or less disklike whereas

low-luminosity objects are more nearly spherical. What is generally required is that the ratio (scale height)/HX be a decreasing function of HX.

In practice it is possible that all three of the above geometrical mechanisms are operating in Seyfert galaxies. With a much larger hard X-ray selected sample one could study the dependence of $H\beta/HX$ on b/a (as in Fig. 3) in different HX ranges. This could elucidate the geometry of the emission line regions as a function of HX.

c) Problems and Speculations

i) New Standard Candles?

Whenever one discovers a relationship between observables that is a function of luminosity, as in Figures 4–8, there is the potential that it may be useful as a distance indicator. Before any of the relations found here can be used, it will be necessary to establish the dispersion on the relation. Of course, it may also be the case that the form of the relation is itself a function of cosmological epoch.

ii) Is There Only One Kind of Seyfert Galaxy?

In terms of the concept of “intermediacy” as promoted by Osterbrock and his colleagues in many papers (Osterbrock and Koski 1976; Osterbrock 1979), we have argued that NELGs are, so to say, Seyfert 1.9 galaxies, and that at least some Type 2’s are Seyfert 1.98, and so on (the exact numbers are of course unimportant). But many Type 2’s may be quite different objects, whose current upper limits happen to fall in the right region of our graphs. Hard X-ray measurements of Type 2 Seyferts must be a top priority for future observations, to decide whether they really are extremely heavily obscured Type 1 Seyferts. Here we suggest two such possibilities: a dense cluster of X-ray binaries, and a “glowing embers” model.

Kriss, Canizares, and Ricker (1980) have pointed out that luminosities of the order $SX = 10^{41}$ ergs s^{-1} may be explained by the presence of $\sim 10^4$ X-ray binaries in the galactic nucleus (perhaps, for instance, brought about by a burst of star formation). Here we also point out that the emission-line spectrum would not be like a normal H II region, but probably in fact more similar to the narrow line spectrum of Type 1’s, with photoionization by a wide range of energetic photons from UV through X-rays. The main argument against this is that the width of even the “narrow” lines is of the order 500 km s^{-1} , which is much larger than that found normally in the nuclear regions of galaxies.

It may also be that some Type 2’s are Seyfert galaxies whose central source has “switched off.” In this case, the broad lines would disappear within a few weeks, but the narrow lines would persist for $\sim 10^3$ years. Seyfert nuclei may switch from “high state” to “low state”

quite frequently. One might then expect to find some narrow-line quasars (as one might also from the inclination effect). In both cases, however, they may be rarer than narrow-line objects at lower luminosities. For 3CR radio galaxies, where the giant radio structure is a record of past activity, Hine and Longair (1979) suggest that more luminous objects spend a larger fraction of their time in the ON state. Likewise, if as suggested in § IVb(ii), the axial ratio of the emission line regions is a function of HX, such that high-luminosity objects are closer to being disklike, then a much smaller solid angle of possible viewing directions is effectively edge-on than is the case for low-luminosity objects, so that edge-on quasars are relatively rare.

The discovery of a narrow emission line quasar has recently been reported by Stocke *et al.* (1982). Values reported by Stocke *et al.* (1982) for SX, O III, and $H\beta$ are consistent with our relations. Many more such objects would be necessary to explore the consequences of the above ideas.

iii) What Are the Underlying Physical Parameters?

It is clear that HX relates to something fundamental other than just telling us the number of ionizing photons. The data presented in this paper do not directly address the question of the origin of the nonthermal continuum. However, any complete theory of Seyfert galaxies must explain why the structure of the emission line regions is so closely related to the power of the continuum source.

We can pose these questions more precisely in the context of the currently popular models involving accretion onto massive black holes (see, e.g., Rees 1978). We then expect that HX is simply proportional to the mass of the black hole and the accretion rate. If black holes accrete at the Eddington limit, then the accretion rate is not a free parameter. The basic problem our data then pose is why condensations in the accretion flow occur with a larger filling factor and/or within a larger region for smaller black holes.

There is evidence for a second free parameter distinct from HX. Most of the graphs we have presented have a scatter of around an order of magnitude. The correlations are only visible because of the large number of galaxies and their wide range of luminosities. We have information on the scatter caused by observational error and variability, as many of the numbers in Table 2 have come from several independent sources. We find that typically independent observations can differ by a factor 2–3 at most. This tells us that two (or possibly more) independent parameters must be specified in any attempted theoretical explanation of Seyfert galaxies. One of them is closely linked to HX, and others are as yet unknown.

The scatter we observe is somewhat larger than that seen by Yee (1980) between what he calls L_{NT} and $H\beta$.

We suspect that there are two reasons for this. The first is that usually Yee (1980) derived L_{NT} and $H\beta$ from the same observation, thus removing some of the scatter we have due to variability. The second reason is that L_{NT} , which is basically the continuum luminosity between 2800 Å and 3500 Å, probably has a large contribution from the Balmer continuum (Malkan and Sargent 1982). This contribution should be tightly correlated with $H\beta$.

Extreme examples of the scatter may provide clues to an extra parameter. NGC 6814, NGC 4051 and NGC 3227 all have low L10, L3.5, and O III compared to typical objects at the same HX or SX. Interestingly, both NGC 6814 and NGC 4051 have reported instances of extremely fast X-ray variability (i.e., on a time scale of minutes; Tennant *et al.* 1981; Marshall *et al.* 1980). A study of 30 galaxies with HEAO A-2 found no other instances of such very fast variability (Tennant *et al.* 1982, in preparation).

V. CONCLUSION

There may be several different ways to make something that looks like a Type 2 Seyfert nucleus, as we have pointed out in the previous section. However, it seems likely that, in fact, there is only one kind of Seyfert galaxy. Intrinsically less luminous examples do not simply look like weaker copies of bright Seyfert galaxies because of the subtle geometrical effects of obscuration which produce qualitatively different appearances at various intrinsic luminosities.

The first stage of understanding of a phenomenon is often taxonomical, so that a qualitative continuum is first recognized as a finite number of categories—this galaxy either has or does not have broad emission lines; this Seyfert either is or is not an X-ray source, etc. We urge the most sensitive possible search for broad wings

on $H\alpha$, and for hard X-ray emission, from Type 2 Seyferts.

The observed range of qualitative appearances may be explained by a photoionization model if the structure of the emission line regions is a function of direction and intrinsic luminosity. Probably both BLR and NLR have an oblate configuration. We hesitate to call this a disk as it may well be rather more like a pumpkin. Indeed, it may be that the axial ratio of the nuclear region is a function of intrinsic luminosity and/or the angular momentum of the nuclear material. We also require that the quantity fH/r (f =filling factor, r =cloud size, H =cloud region size) be a function of intrinsic luminosity for the BLR. For the NLR it is likely either that f/r is a function of intrinsic luminosity or that $f \propto R^{-3}$, where R is the radial distance from the X-ray source.

We urge theoretical consideration of these possibilities.

We would like to thank several colleagues who have provided their data in advance of publication: Irene Cruz-González, Jerry Kriss, Bill Ku, Frank Marshall, Martin Ward, and Bill Keel for permission to reproduce Figure 1. We have also benefited enormously from discussions with several colleagues, especially Claude Canizares, Jerry Kriss, Julian Krolik, and Richard Mushotzky.

Note added in manuscript 1982 January 11.—G. A. Kriss (private communication) informs us that the correct value of SX for Mrk 142 should be 1.2×10^{43} ergs s^{-1} . This does not affect any of our conclusions. He also informs us that *Einstein Observatory* HRI observations confirm the identification of Mrk 279 with 2A 1348+700.

REFERENCES

- Adams, T. F. 1977, *Ap. J. Suppl.*, **33**, 19.
 Adams, T. F., and Weedman, D. W. 1975, *Ap. J.*, **199**, 19.
 Anderson, K. S. 1970, *Ap. J.*, **162**, 743.
 Bahcall, J. N., Bahcall, N. A., Murray, S., and Schmidt, M. 1975, *Ap. J. (Letters)*, **199**, L9.
 Boksenberg, A., *et al.* 1975, *M.N.R.A.S.*, **173**, 381.
 Bradt, H. V., Burke, B. F., Canizares, C. R., Greenfield, P. E., Kelley, R. L., McClintock, J. E., van Paradijs, J., and Koski, A. T. 1978, *Ap. J. (Letters)*, **226**, L111.
 Canizares, C. R., McClintock, J. E., and Ricker, G. R. 1978, *Ap. J. (Letters)*, **226**, L1.
 Carswell, R. F., and Ferland, G. J. 1980, *M.N.R.A.S.*, **191**, 55.
 Cooke, B. A., *et al.* 1978, *M.N.R.A.S.*, **182**, 489.
 Danziger, I. J., Fosbury, R. A. E., and Penston, M. V. 1977, *M.N.R.A.S.*, **179**, 41p.
 Davidson, K., and Netzer, H. 1979, *Rev. Mod. Phys.*, **51**, 715.
 de Bruyn, A. G., and Sargent, W. L. W. 1978, *A.J.*, **83**, 1257.
 de Vaucouleurs, G., de Vaucouleurs, A., and Corwin, H. 1976, *Second Reference Catalogue of Bright Galaxies* (Austin: University of Texas).
 Dower, R. G., Griffiths, R. E., Bradt, H. V., Doxsey, R. E., and Johnston, M. D. 1980, *Ap. J.*, **235**, 355.
 Elvis, M. 1978, Ph.D. thesis, University of Leicester.
 Elvis, M., Maccacaro, T., Wilson, A. S., Ward, M. J., Penston, M. V., Fosbury, R. A. E., and Perola, G. C. 1978, *M.N.R.A.S.*, **183**, 159.
 Glass, I. S. 1978, *M.N.R.A.S.*, **184**, 85p.
 ———. 1979, *M.N.R.A.S.*, **186**, 29p.
 Griffiths, R. E., Doxsey, R. E., Johnston, M. D., Schwartz, D. A., Schwarz, J., and Blades, J. C. 1979, *Ap. J. (Letters)*, **230**, L21.
 Harwit, M., and Pacini, F. 1975, *Ap. J. (Letters)*, **200**, L127.
 Hine, R. G., and Longair, M. S. 1979, *M.N.R.A.S.*, **188**, 111.
 Holmberg, E. 1975, in *Stars and Stellar Systems*, Vol. 9, *Galaxies and the Universe*, ed. A. and M. Sandage and J. Kristian (Chicago: University of Chicago Press), p. 123.
 Holt, S. S., Mushotzky, R. F., Becker, R. H., Boldt, E. A., Serlemitsos, P. J., Szymkowiak, A. E., and White, N. E. 1980, *Ap. J. (Letters)*, **241**, L13.
 Jenkins, E. B., and Savage, B. D. 1974, *Ap. J.*, **187**, 243.
 Keel, W. C. 1980, *A.J.*, **85**, 198.
 Khachikian, E. Ye., and Weedman, D. W. 1974, *Ap. J.*, **192**, 581.
 Koski, A. T. 1978, *Ap. J.*, **223**, 56.
 Kriss, G. A., Canizares, C. R., and Ricker, G. R. 1980, *Ap. J.*, **242**, 492.
 Ku, W. H.-M., Helfand, D. J., and Lucy, L. B. 1980, *Nature*, **288**, 323.

- Kwan, J., and Krolik, J. H. 1979, *Ap. J. (Letters)*, **233**, L91.
Maccacaro, T., Perola, G. C., and Elvis, M. 1982, *Ap. J.*, **255**, in press.
Malkan, M. A., and Sargent, W. L. W. 1982, *Ap. J.*, **254**, in press.
Marshall, F. E., Becker, R. H., Holt, S. S., and Mushotzky, R. F. 1980, *Bull. AAS*, **12**, 796.
Marshall, F. E., Boldt, E. A., Holt, S. S., Mushotzky, R. F., Praydo, S. H., Rothschild, R. E., and Serlemitsos, P. J. 1979, *Ap. J. Suppl.*, **40**, 657.
Marshall, N., and Warwick, R. S. 1979, *M.N.R.A.S.*, **189**, 37p.
Marshall, N., Warwick, R. S., and Pounds, K. A. 1981, *M.N.R.A.S.*, **194**, 987.
McAlary, C. W., McLaren, R. A., and Crabtree, D. R. 1979, *Ap. J.*, **234**, 471.
McClintock, J. E., van Paradijs, J., Remillard, R. A., Canizares, C. R., Koski, A. T., and Véron, P. 1979, *Ap. J.*, **233**, 809.
McHardy, I. M., Lawrence, A., Pye, J. P., Pounds, K. A. 1981, *M.N.R.A.S.*, **197**, 893.
Mushotzky, R. F. 1982, *Ap. J.*, **256**, in press.
Mushotzky, R. F., Marshall, F. E., Boldt, E. A., Holt, S. S., and Serlemitsos, P. J. 1980, *Ap. J.*, **235**, 377.
Neugebauer, G., Becklin, E. E., Oke, J. B., and Searle, L. 1976, *Ap. J.*, **205**, 29.
Osmer, P. S., Smith, M. G., and Weedman, D. W. 1974, *Ap. J.*, **192**, 279.
Osterbrock, D. E. 1977, *Ap. J.*, **215**, 733.
———. 1978, *Phys. Scripta*, **17**, 285.
———. 1979, *A.J.*, **84**, 901.
Osterbrock, D. E., and Koski, T. 1976, *M.N.R.A.S.*, **176**, 61p.
Penston, M. V., Penston, M. J., Selmer, R. A., Becklin, E. E., and Neugebauer, G. 1974, *M.N.R.A.S.*, **169**, 357.
Phillips, M. M., Feldman, F. R., Marshall, F. E., and Wamsteker, W. 1979, *Astr. Ap.*, **76**, L14.
Pineda, F. J., Delvalle, J. P., Grindlay, J. E., and Schnopper, H. W. 1980, *Ap. J.*, **237**, 414.
Puschell, J. J. 1981, *A.J.*, **86**, 16.
Rees, M. J. 1978, *Phys. Scripta*, **17**, 193.
Rieke, G. H. 1978, *Ap. J.*, **226**, 550.
Rubin, V. C. 1978, *Ap. J. (Letters)*, **224**, L55.
Schnopper, H. W., Davis, M., Delvalle, J. P., Geller, M. J., and Huchra, J. P. 1978, *Nature*, **275**, 719.
Shuder, J. M. 1980, *Ap. J.*, **240**, 32.
Siegel, S. 1956, *Non-parametric Statistics for the Behavioral Sciences* (New York: McGraw-Hill).
Stark, J. P., Bell Burnell, J., and Culhane, J. L. 1978, *M.N.R.A.S.*, **182**, 23p.
Stein, W. A., and Weedman, D. W. 1976, *Ap. J.*, **205**, 44.
Steiner, J. E. 1981, *Ap. J.*, **250**, 469.
Stocke, J., Liebert, J., Maccacaro, T., Griffiths, R. E., and Steiner, J. E. 1982, *Ap. J.*, **252**, 69.
Tananbaum, H., et al. 1979, *Ap. J. (Letters)*, **234**, L9.
Tananbaum, H., Peters, G., Forman, W., Giacconi, R., and Jones, C. 1978, *Ap. J.*, **223**, 74.
Tennant, A. F., Mushotzky, R. F., Boldt, E. A., and Swank, J. H. 1981, *Ap. J.*, **251**, 15.
Véron, P., Lindblad, P. O., Zuiderwijk, E. J., Véron, M. P., and Adam, G. 1980, *Astr. Ap.*, **87**, 245.
Vorontsov-Velyaminov, B. A., et al. 1962–1974, *Morphologicheskii Katalog Galaktik* (Moscow: Sternberg Institute), Vols. 1–5 (MCG).
Ward, M. J. 1979, Ph.D. thesis, University of Sussex.
Ward, M. J., Penston, M. V., Blades, J. C., and Turtle, A. J. 1980, *M.N.R.A.S.*, **193**, 563.
Ward, M. J., and Wilson, A. S. 1978, *Astr. Ap.*, **70**, L79.
Ward, M. J., Wilson, A. S., Penston, M. V., Elvis, M., Maccacaro, T., and Tritton, K. P. 1978, *Ap. J.*, **223**, 788.
Warwick, R. S., and Pye, J. P. 1979, *M.N.R.A.S.*, **187**, 905.
Watson, M. G., and Griffiths, R. E. 1980, *Bull. AAS*, **12**, 873.
Weedman, D. W. 1977, *Ann. Rev. Astr. Ap.*, **15**, 69.
Wilson, A. S. 1979, *Proc. R. Soc. London, A*, **366**, 461.
Wilson, A. S., and Penston, M. V. 1979, *Ap. J.*, **232**, 389.
Wilson, A. S., Penston, M. V., Fosbury, R. A. E., and Boksenberg, A. 1976, *M.N.R.A.S.*, **177**, 673.
Yee, H. K. C. 1980, *Ap. J.*, **241**, 894.

MARTIN ELVIS: Harvard-Smithsonian Center for Astrophysics, 60 Garden Street, Cambridge, MA 02138

ANDREW LAWRENCE: Royal Greenwich Observatory, Herstmonceux Castle, Hailsham, Sussex BN27 1RP, England